Design methodology of an active back-support exoskeleton with adaptable backbone-based kinematics

Loris Roveda [a,*], Luca Savani [b], Sara Arlati [c], Tito Dinon [c], Giovanni Legnani [b,c], Lorenzo Molinari Tosatti [c]

[a] *Istituto Dalle Molle di Studi sull'Intelligenza Artificiale (IDSIA), Scuola Universitaria Professionale della Svizzera Italiana (SUPSI), Universitá della Svizzera Italiana (USI) IDSIA-SUPSI, Manno, Switzerland*
[b] *University of Brescia, Department of Mechanical and Industrial Engineering, Brescia, Italy*
[c] *Consiglio Nazionale delle Ricerche (CNR), Istituto di Sistemi e Tecnologie Industriali per il Manifatturiero Avanzato (STIIMA), Manno, Italy*

A B S T R A C T

Manual labor is still strongly present in many industrial contexts (such as aerospace industry). Such operations commonly involve onerous tasks requiring to work in non-ergonomic conditions and to manipulate heavy parts. As a result, work-related musculoskeletal disorders are a major problem to tackle in workplace. In particular, back is one of the most affected regions. To solve such issue, many efforts have been made in the design and control of exoskeleton devices, relieving the human from the task load. Besides upper limbs and lower limbs exoskeletons, back-support exoskeletons have been also investigated, proposing both passive and active solutions. While passive solutions cannot empower the human's capabilities, common active devices are rigid, without the possibility to track the human's spine kinematics while executing the task. The here proposed paper describes a methodology to design an active back-support exoskeleton with backbone-based kinematics. On the basis of the (easily implementable) *scissor hinge mechanism*, a one-degree of freedom device has been designed. In particular, the resulting device allows tracking the motion of a reference vertebra, *i.e.*, the vertebrae in the correspondence of the connection between the scissor hinge mechanism and the back of the operator. Therefore, the proposed device is capable to adapt to the human posture, guaranteeing the support while relieving the person from the task load. In addition, the proposed mechanism can be easily optimized and realized for different subjects, involving a subject-based design procedure, making possible to adapt its kinematics to track the spine motion of the specific user. A prototype of the proposed device has been 3D-printed to show the achieved kinematics. Preliminary tests for discomfort evaluation show the potential of the proposed methodology, foreseeing extensive subjects-based optimization, realization and testing of the device.

1. Introduction

Manual operations are still highly present in the industrial context (Roveda et al., 2017). Human operators have often to execute onerous tasks (*e.g.*, in non-ergonomic conditions, lifting heavy loads, etc.). As a results, work-related musculoskeletal disorders are a huge issue to be addressed in industrial contexts (Wang et al., 2017; Liu et al., 2019a; Bao et al., 2020). In particular, back-pain is the most recorded work-related pathology (Ibrahim et al., 2019), having only in the United States an associated cost of 100 billions $ per year (Katz, 2006).

Based on the Industry 4.0 paradigm (Lu, 2017), human-robot collaboration is widely investigated to relieve the human operator from non-ergonomic, onerous and repetitive applications (Hentout et al., 2019; Liu et al., 2019b). In this field, two main solutions can be identified from the state of the art: (i) collaborative robots (Bragança et al., 2019) and (ii) wearable robots (Yang et al., 2017). While collaborative robots can be exploited for repetitive applications

(Vicentini et al., 2020), wearable robots represent a highly-flexible solution to be exploited for added-value operations (De Looze et al., 2016; Bogue, 2018). Many solutions have been developed to empower and assist the human operator, spanning from upper limbs exoskeletons (Spada et al., 2017; Blanco et al., 2019; Pacifico et al., 2020) to lower limbs exoskeletons (Guncan and Unal, 2018; Luger et al., 2019; Wijegunawardana et al., 2019). In order to solve the issue related to back-pain disorders, back-support exoskeletons represent the optimal solution in order to correctly redistribute the spinal load, improving the ergonomics while relieving the human operator from the load. In the next Section, state of the art related to such type of exoskeletons is analyzed.

1.1. Back-support exoskeletons solutions

The need to solve work-related back-pain disorders is highly demanded in the industrial context. Many attentions have been targeted

---

to such topic, *e.g.*, analyzing the trunk muscle fatigue during dynamic lifting and lowering (Shin and Kim, 2007), investigating the possibility to correct the task execution exploiting real-time bio-feedback signals (Boocock et al., 2019), proposing a passive lower limbs exoskeleton to assist the human during squat lifting (Wehner et al., 2009), studying the elongation of the surface of the spine during lifting and lowering for exoskeleton design purposes (Huysamen et al., 2018a). Back-support exoskeletons are under investigation in order to support and relieve the human operator from heavy loads and non ergonomic postures. *Ad hoc* solutions have been addressed, optimizing the design parameters on the basis of the specific task (Manns et al., 2017). Passive and active solutions can be identified from the state of the art analysis. Considering passive solutions, the following works can be found. In (Näf et al., 2018) a passive back-support exoskeleton has been developed. The proposed solution is based on a mechanism composed by flexible beams running in parallel to the spine, allowing to achieve a large range of motion while lowering torque requirements around the lumbo-sacral joint. In (Li et al., 2019) a trunk exoskeleton has been designed on the basis of multibody dynamic modeling. In (Baltrusch et al., 2020) the SPEXOR passive spinal exoskeleton is described. Works investigating the passive exoskeletons performance have been proposed, analyzing the achieved results in terms of user performance (Bosch et al., 2016; Baltrusch et al., 2018; Hensel and Keil, 2019; Koopman et al., 2019; Madinei et al., 2020). Solutions available on the market can also be found (Suitx and https://www.suitx., 2020; Exobionics and https://eksob, 2020; Lockheed martin and https://, 2020; Comau mate and https://www.c, 2020; Aldak and https://exoskeleto, 2020; Backx and https://ex-oskeleto, 2020; Flx-ergoskeleton and https:/, 2020; h-wex and https://exoskeleto, 2020; Laevo v2 and https://exoskel, 2020; V22 ergoskeleton and https:/, 2020; Hyundai vex and https://www., 2020). On the other hand, considering active solutions, the following works can be found. In (Naruse et al., 2003) a back-support device for lower back flexion and extension has been proposed for heavy load carrying applications. In (Toxiri et al., 2017a) low-back exoskeleton has been proposed to support manual material handling in industrial contexts. In (Ko et al., 2018) a waist exoskeleton has been proposed, implementing a wire-driven single actuator mechanism. In (Zhang and Huang, 2018) an exoskeleton to provide back-support and to reduce lumbar spine compression is proposed exploiting serial elastic actuators (SEA). In (Lanotte et al., 2018) a pelvis orthosis has been proposed to assist workers during lifting operations. Works investigating the active exoskeletons performance have been proposed, analyzing the achieved results in terms of user performance (Toxiri et al., 2017b; Huysamen et al., 2018b). Solutions available on the market can be found in this case too (Awn and https://exoskeletonr, 2020; Hal lumbar support and https, 2020; Muscle suit and https://exos, 2020; Atlas and https://exoskeleto, 2020).

In general, while passive solutions are commonly characterized by lower costs and easier implementation, active exoskeletons are generally preferred due to the possibility to actively assist the human during the task execution. However, the available solutions from the state of the art and from the market are commonly characterized by rigid structures, limiting the range of motion of the human and being tailored for very specific applications. The only available active solution with non-rigid structure is proposed in Yang et al. (2019), where a spine-inspired continuum soft exoskeleton has been proposed for stoop lifting assistance. The proposed device, however, is characterized by a complex kinematics, which is difficult to be replicated/adapted to different users. Therefore, there is still the need to design a kinematically advanced solution with a structure adaptable to both the operator anatomical features, and to the task to be accomplished.

1.2. Paper contribution

Starting from the work in Mauri et al. (2019), the here presented paper proposes a methodology for the design of an active back-support

exoskeleton with backbone-based kinematics, aiming at assisting the human operator in onerous tasks. Exploiting an opportunely designed *scissor hinge mechanism*, a one-degree of freedom (DoF) device has been studied (Fig. 1). The spatial displacement of a reference vertebra (*i.e.* the one in the correspondence of the connection between the scissor hinge mechanism and the back of the operator) is considered for the design of the mechanism, thus ensuring that the device follows its motion during the task execution. Therefore, the proposed device adapts to the human anatomical characteristics, assisting the human operator in the complete set of postures assumed during the operations. Due to its simple implementation and scalability, the scissor hinge mechanism allows to easily re-design the device to adapt to different users exploiting a parametric design. The kinematics of the device has been derived on the basis of the acquired subject-specific backbone kinematics, recorded using a stereophotogrammetric motion capture system (Vicon camera system and http, 2020). Such data has been post-processed in order to extract the motion of the reference vertebra, making possible to design the scissor hinge mechanism. A prototype of the proposed back-support exoskeleton has been 3D-printed to show its simple implementation. The validation of its kinematics capabilities and discomfort have been performed with preliminary tests. Such tests are not exhaustive and do not claim to validate the complete performance of the designed prototype. The main aim of such tests have been the validation of the proposed design methodology, to understand its suitability and its potential. Having achieved a satisfactory design, future work will extensively address subjects-based optimization, realization and testing of the device to evaluate its full performance.

1.3. Paper layout

The paper is structured as follows: Section 2 proposes the user-specific backbone kinematics analysis, describing the adopted setup for its motion acquisition and its elaboration to extract the reference vertebra motion for the device design purposes; Section 3 proposes the design of the back-support exoskeleton with a focus on the scissor hinge mechanism for the backbone-based kinematics; Section 4 details the conclusions and future works.

2. User-specific reference vertebra motion analysis

In this Section, the backbone kinematics is analyzed in order to derive the user-specific back-support exoskeleton kinematics design. In the following, the backbone structure is introduced, the methodology for the vertebrae motion acquisition is detailed, and the reference vertebrae motion elaboration is described.

2.1. Backbone structure

2.1.1. The backbone
The backbone (Fig. 2) is part of the axial skeleton and goes from the base of the skull to the pelvis. In humans, it is made of articulating vertebrae, whose function is to give strength and flexibility to the spinal column. Vertebrae support the head and the trunk against gravity, but also allow for the flexion, the extension and the torsion of both the neck and the upper body. Another important function of the backbone is to protect the spinal cord which travels within the spinal canal, *i.e.*, a series of central holes within each vertebra. In adults, the backbone is generally composed on average by 33 vertebrae: the upper 24 are articulating and separated by intervertebral disks, whereas the remaining 9 are fused in the sacrum and in the coccyx. The vertebrae are named according to the region of the backbone to which they belong to; normally, there are 7 cervical (C1–C7), 12 thoracic (T1-T12), 5 lumbar (L1-L5), 5 sacral (S1–S5) and 3 to 5 coccygeal vertebrae.

2.1.2. Vertebrae
All the vertebrae share the same anatomical features, though they

Fig. 1. Active adaptive back-support exoskeleton with backbone-based kinematics.
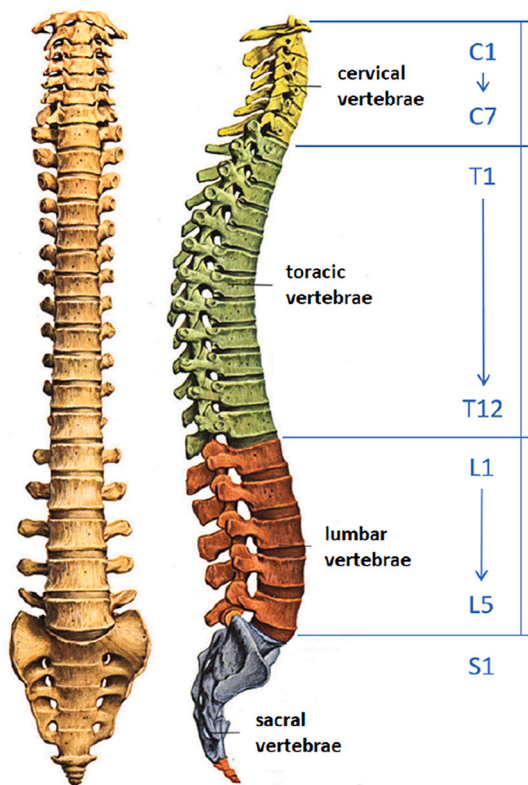
Fig. 2. Spine structure for the kinematics analysis.

may have some differences. A typical vertebra is constituted by the vertebral body and the vertebral arch. The body is anterior and composed of cancellous bone covered by a thin coating of cortical bone,

i.e., the hard and dense type of bone tissue. This part of the vertebra has the aim of supporting the head and the trunk weight. The vertebral arch, instead, is posterior. It is formed by a pair of pedicles and a pair of laminae, and supports seven processes, four articular, two transverse, and one spinous. The articular processes are characterized by the presence of facets joints covered with cartilage, and serve the purpose of fitting with the adjacent vertebrae. The transverse processes project from either side and constitute the attachment of muscles and ligaments, in particular the intertransverse ligaments. The spinous process points dorsally and caudally and, as for the transverse processes, serves for ligament and muscles' attachment. The spinous processes are the bones that generally can be felt through the skin. The vertebral arch and the vertebral body enclose the foramen, *i.e.*, the cavity that contains the spinal cord. The spinal cord ends in the lumbar region; therefore, the fused vertebrae do not contain the vertebral foramen. The spinal nerves leave the spinal cord through small holes called intervertebral foramina that lie in-between two adjacent vertebrae.

2.1.3. Intervertebral discs

Intervertebral discs lie between adjacent vertebrae in the vertebral column, with the exception of C1 and C2 vertebrae whose anatomy is different to permit neck rotation. Intervertebral discs are fixed on the rough inferior and superior end-plates of the vertebral bodies; they are made of an outer fibrous ring made of collagen, the annulus fibrosus, which surrounds the nucleus pulposus, a sort of gel containing suspended loose fibers.

The structure of each disk allows the spinal column to withstand the compressive forces occurring during walking or jumping that otherwise would result in the fracture of the vertebrae, or into excessive vibrations transmitted to the brain. Each disc also forms a fibrocartilaginous joint (called symphysis) that allows for the relative rotation between adjacent vertebrae, and for limited movements in the coronal and in the sagittal planes.

2.2. Backbone kinematic model

The following assumptions have been made in order to define the kinematic model of the backbone:

- considering the backbone structure in Fig. 2, the design of the back-support exoskeleton does not consider the cervical vertebrae. In fact, the cervical vertebrae do not affect the kinematics and dynamics of the model, as the exoskeleton is not expected to extend past C7;
- the backbone allows to move in the coronal and in the sagittal planes; additionally, it can also rotate around its central axis. This model considers only the movement in the sagittal plane. In fact, the spinal range of motion that we expect to measure occurs mainly in this plane. Anyway, the design of the exoskeleton will allow small movements in the other two directions, as elastic elements will be placed between the device and the human operator. These elements should also contribute in reducing the stiffness of the whole exoskeleton, and thus the feeling of being limited or constricted. It is important to point out that the proposed design was aimed to keep the mechanical structure of the exoskeleton as simple as possible, specifically addressing lifting and transportation tasks (*i.e.*, tasks in which back flexion-extension motion is expected to be significantly more marked than lateral flexion, or axial rotation);
- the design of the exoskeleton does not consider the potential elongation of the backbone due to the lifting of a heavy object; in between a limited range of (acceptable) weights, this assumption represents a good approximation (Huysamen et al., 2018a).

The experiment described in the next sub-paragraphs aims at evaluating the displacement of the vertebrae and the distances between spinous processes during the performance of two lifting tasks. This information is needed to design an exoskeleton able to adapt the anatomical characteristics of each operator.

2.2.1. Equipment

A stereophotogrammetric system (Vicon camera system and http, 2020) has been used to capture vertebrae motion (Fig. 3). Such motion capture system was composed by 8 infra-red cameras (Vicon Vero 2.2) able to capture in real-time the position of reflective markers in the 3D space. VICON Nexus software (version 2.7.1) was used to calibrate the working area, and to collect the motion data. Data were acquired using a sampling frequency of 100 Hz.

All the experiments have been carried out in the Lecco premises of CNR-STIIMA (Lecco, LC, Italy).

2.2.2. Protocol

The protocol used in this study recalls what reported in Huysamen et al. (2018a). Nineteen markers have been placed on the back of the subject in correspondence of vertebrae spinous processes, from C7 to S1
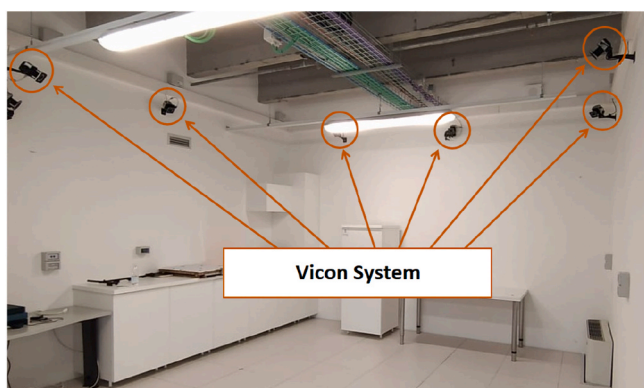
(Fig. 4). Markers' positioning has been done by an expert operator, who also checked that during the forward flexion, markers kept their position relative to the vertebra; this was made to ensure data accuracy, and to avoid recording unwanted movements due to the viscoelastic nature of the skin. After markers placement, the subject was asked to lift an object whose weight was negligible using two different strategies: through a *squat, i.e.*, the correct movement, and through a *stoop, i.e.*, a movement that implies the forward bending, and that is usually discouraged as it causes higher spinal loads (Bazrgari et al., 2007). Each lifting strategy has been applied three times, for a total of six trials.

2.3. Data elaboration

Data have been analyzed in Matlab 2019b using *ad-hoc* scripts.

2.3.1. Data visualization

The recorded 3D positions for all the 19 markers, plotted in the sagittal plane are shown in Fig. 5. Each ∗ represents the position of a specific vertebra in the sagittal plane during the protocol execution (squat phase). The black lines connecting the ∗ represent the backbone configuration throughout the movement.

2.3.2. Data processing

In order to make use of the data shown in Fig. 5, three main data processing steps are needed:

Step 1 reference frame definition. The origin of the reference frame used for all the vertebrae motion data is positioned in the correspondence of the last lumbar vertebra L5;

Step 2 down-sampling of the recorded data. In order to improve usability of the data, a down-sampling from 100 Hz to 20 Hz has been performed;

Step 3 filtering of the acquired data. In order to avoid noise in the recorded vertebrae positions, data filtering has been performed. The filtering frequency has been imposed equal to 5 Hz.

The obtained post-processed data related to the motion of the

Fig. 3. Test environment.
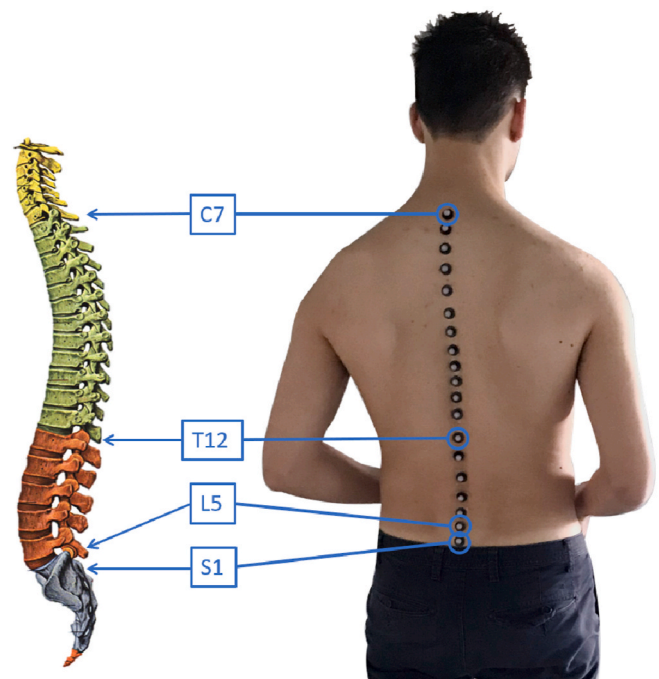
Fig. 4. Marker placement on the back of the subject for backbone motion capture.
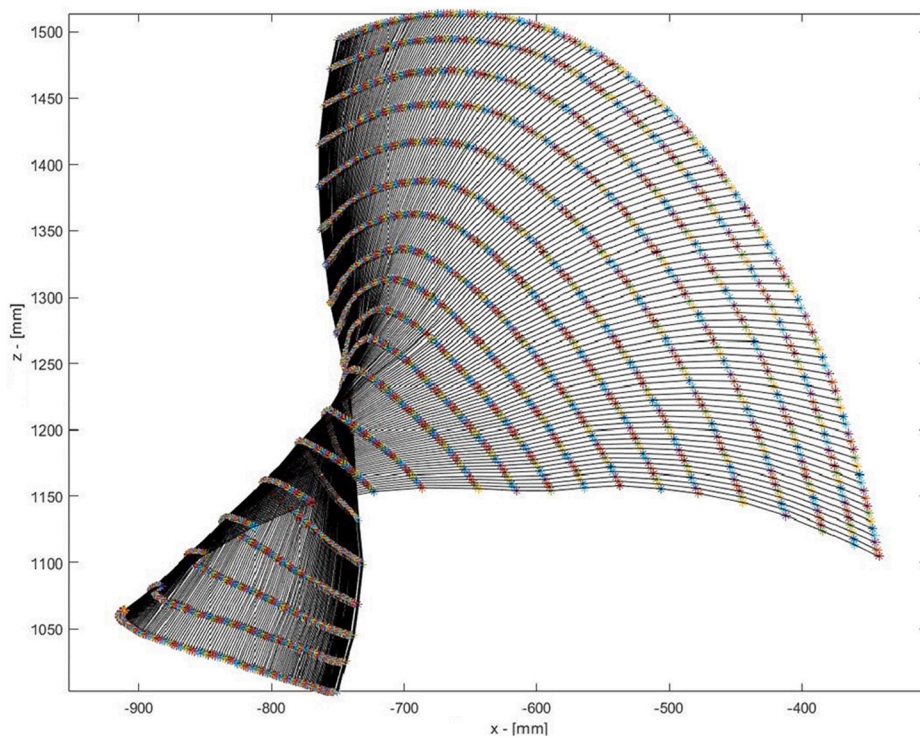
Fig. 5. Recorded vertebrae positions in the sagittal plane during the protocol execution (squat phase).

vertebrae are shown in Fig. 6.

2.3.3. Approximated vertebrae motion path

On the basis of the acquired and processed data, it was possible to derive the approximated motion path followed by each vertebra during the proposed protocol execution. More in details, as shown in Fig. 7, it has been possible to define an approximated circular path for the vertebrae motion. It could be highlighted that the center of the resulting circumferences is approximately overlapped (except for the last 5 vertebrae). Such circular path can be obtained for all the six acquisitions done in Section 2.2.2, averaging them to compute the final approximation. Such approximation has been used in order to design the back-support exoskeleton kinematics.
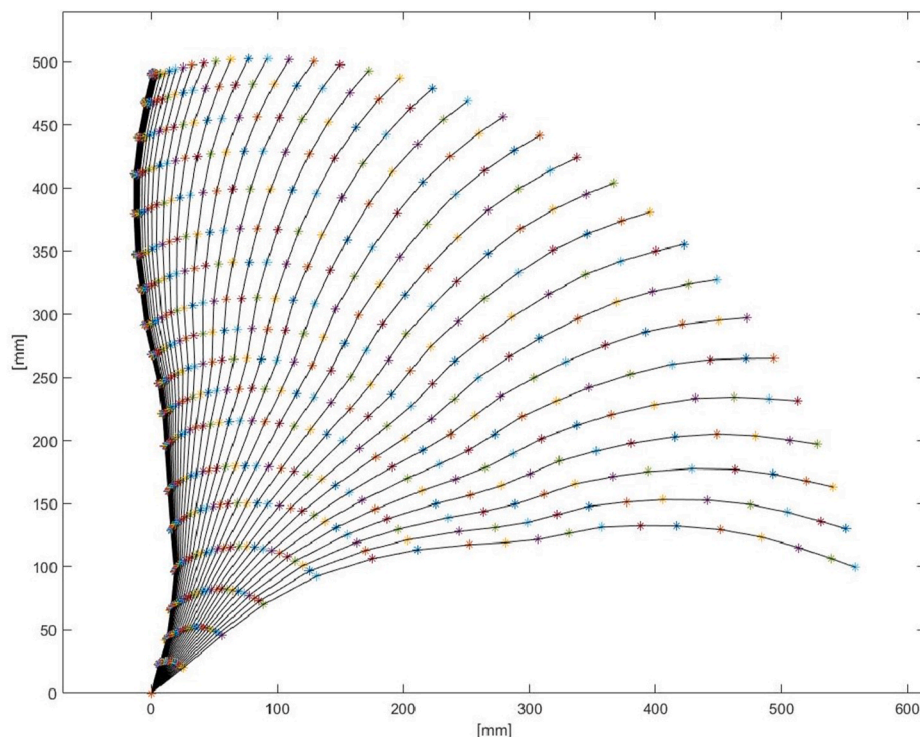
Fig. 6. Post-processed vertebrae motion data.
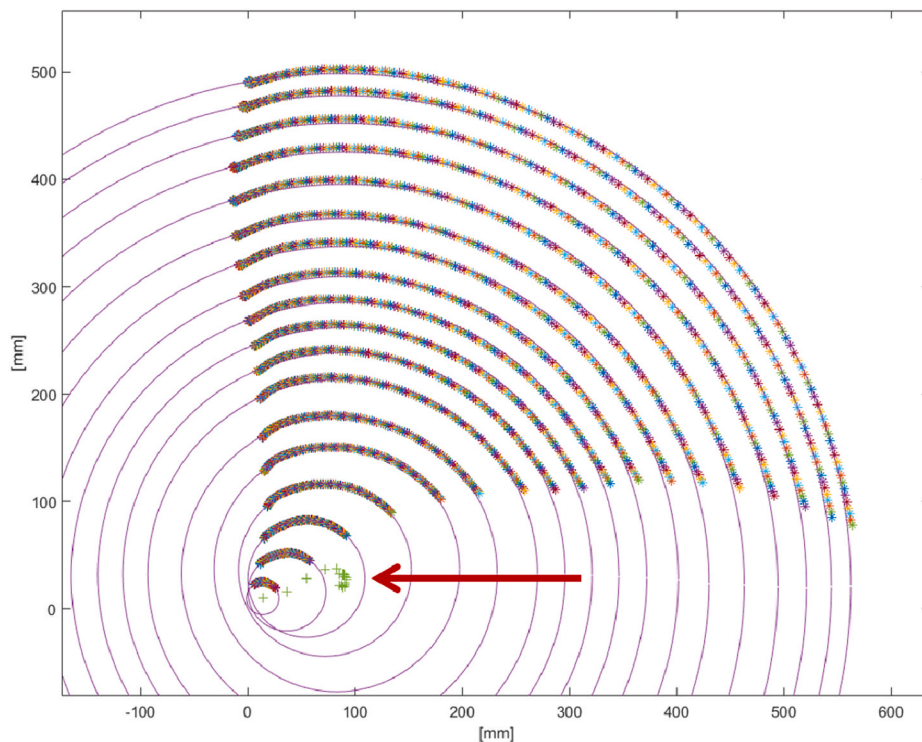
Fig. 7. Circular motion path approximation for the vertebrae. Purple circles highlight the circular approximated paths for each vertebrae, while the * highlight the sampled vertebrae positions. The green markers (highlighted by the red arrow) define the center of the approximated circular paths for each vertebra. (For interpretation of the references to colour in this figure legend, the reader is referred to the Web version of this article.)

Remark 1. The adopted experimental setup is indeed a high-cost setup. The proposed MoCap system can be substituted with another more affordable system, such as an imu-based system.

Remark 2. The presented study has indeed some limitations. The first one is related to the limited number of subjects that tested the device. The second is linked to the experimental methodology that foresaw a limited numbers of trials, and the testing of only a couple of lifting strategies. In the next developments, such limitations will be addressed.

3. Back-support exoskeleton design

In this Section, the design of the back-support exoskeleton is described. Starting from the backbone kinematics derived in Section 2 and by defining the design requirements, the mechanism tracking the motion of the user backbone has been identified. Afterwards, the kinematics of the proposed device was derived. Finally, the optimization of the proposed device has been performed, making possible to 3D-print a prototype of the proposed back-support exoskeleton.

3.1. Design requirements

In order to design the active back-support exoskeleton, the following requirements have been addressed:

- 1 DoF actuated mechanism design: in order to reduce the design complexity and the costs related to the implementation of the proposed solution, a 1-actuated DoF has been considered for the target device. In such a way, only one actuator is required to operate the device, reducing implementation complexity, costs and the dimensions (weight and size) of the device;
- simple user-tailored design and optimization: considering the proposed 1-actuated DoF device, it was not possible to track the complete complex motion of the whole backbone. Instead, a reference vertebra was considered in the correspondence of the connection

between the proposed mechanism and the back of the operator. In fact, the tracking of the motion of a reference vertebra has been the simplest way to implement a simple device following the human's backbone motion, being as transparent as possible (*i.e.*, limiting as much as possible the constraining of the human's motion). As shown in Section 2.3.3, the derived modeling of the vertebrae motion is relatively simple, being easily implementable and trackable by the proposed back-support exoskeleton. Ideally, subjective perception of comfort should be also included into the optimization phase. However, such consideration would require the user to try and evaluate different configurations or different designs of the device. This would result in a huge effort in design, realization and experimental campaigns. Thus, our aim was not to optimize an already existing device, but to focus on an *a-priori* optimization to reach a satisfactory user-tailored design, saving time and costs;

- limited size and weight: in order to improve the ergonomics of the task, the device had to be designed in order to be as lightweight as possible and as small as possible;
- simple and scalable mechanical design: in order to adapt the proposed design to different users, the considered device has been designed to be easily parametrized on the basis of the user-specific backbone kinematics (as detailed in Section 2);
- as described in Section 2, the elongation of the backbone increases of a value equal to Δl (Fig. 8) during flexion. Such elongation is a function of the assumed posture. The designed device had to track such elongation, without constraining the human motion. The load had to be transferred from the spine to the legs, improving the task ergonomics and relieving the human from the task load. The vertebrae separation effect highlighted in Fig. 8 had to be included in the design of the device. Commonly, such effect is neglected in the available devices.
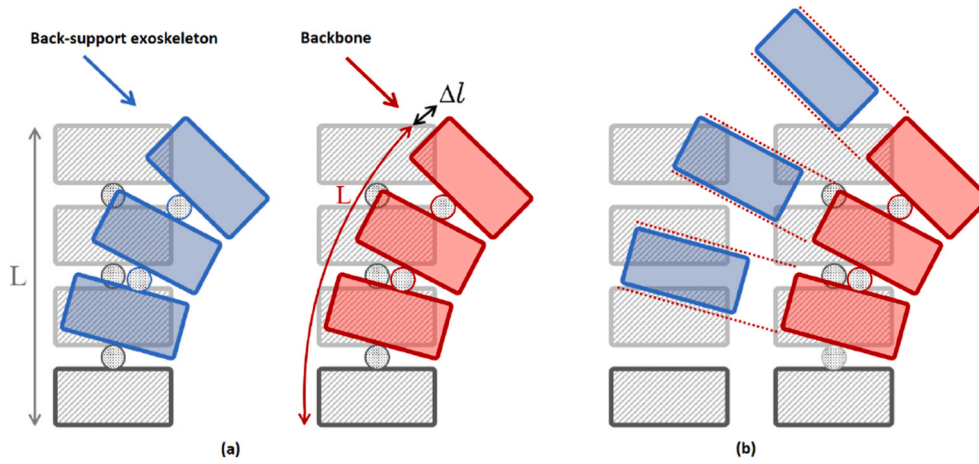
Fig. 8. Backbone elongation during the flexion motion. In red, the backbone elongation is highlighted. In blue, the back-support exoskeleton elongation is highlighted, having on the left side (a) the standard rigid solution, and on the right side (b) the proposed device functionalities. (For interpretation of the references to colour in this figure legend, the reader is referred to the Web version of this article.)

3.2. Scissor hinge mechanism

Following the criteria described in the above Section, especially the fact of limiting the complexity of the device by implementing a single actuated DoF device, the main purpose of this Section is the definition of the kinematics of the mechanism. Instead of tracking the whole complex motion of the user backbone, the kinematics of the device has to be able to track the motion of a reference vertebra (*i.e.*, the one in the correspondence of the connection between the proposed mechanism and the back-support), making possible to adapt the back-support configuration to the human posture.

On the basis of the analysis performed in Section 2 on the vertebrae motion, the mechanism we identified to track the motion of the reference vertebra is the *scissor hinge mechanism* (Chen et al., 2017). Such mechanism is formed by *n* scissor units. Each scissor unit consists of two straight bars, connected to the next one at the intermediate points by a revolute joint (scissor hinge). By altering the location of the scissor hinge, three distinct basic motions are obtained: translational, polar and angular motions (Maden et al., 2011). The main advantage of such a mechanism is related to the high range of motion achieved by a reduced-size mechanism.

The scissor hinge mechanism, opportunely configured, allows tracking a circular path. As detailed in Section 2.3.3, the vertebrae motion path could be approximated with a circular path. Therefore, the proposed mechanism has been designed in order to follow such a circular path, having its center in correspondence of the origin of circle generated by the reference vertebra motion.

3.3. Kinematics of the proposed mechanism

In order to achieve a circular motion of the end-point of the considered scissor hinge mechanism (*i.e.*, the point corresponding to the reference vertebrae), the mechanism configuration in Fig. 9 has been considered. Therefore, the equations describing the kinematics of the mechanism could be derived considering the symbols and the reference frame in Fig. 9, having the horizontal axis *x* coincident to the sagittal axis.

The equations describing the kinematics of the points of interest P_1, P_2 and P_3 (*i.e.*, the revolute joints in P_1 and P_2 and the final point P_3 of the mechanism) could therefore be derived:

$$\begin{cases} z_1 = D \sin(\alpha), \\ x_1 = D \cos(\alpha); \end{cases} \tag{1}$$

Fig. 9. Scissor hinge mechanism configuration to achieve the circular path related to the reference vertebra.

$$\begin{cases} z_2 = D \sin(\alpha) + z_1, \\ x_2 = D \cos(\alpha) - D + x_1; \end{cases} \tag{2}$$

$$\begin{cases} z_3 = L \sin(\alpha + \vartheta') + z_2, \\ x_3 = L \cos(\alpha + \vartheta') - D + x_2. \end{cases} \tag{3}$$

Remark 3. It has to be underlined that, having less or more scissor units, the kinematics of the mechanism can be re-computed reducing or increasing the number of considered revolute joints.

3.4. Optimization of the scissor hinge mechanism

In order to make the proposed scissor hinge mechanism able to track the approximated circular path of the reference vertebra for the specific considered user (*i.e.*, tracking the backbone motion of the reference user to achieve a tailored design for the proposed device), its design has been

set up as an iterative non-linear optimization problem. The vertebra T2 has been considered as the reference one, since it is considered that the connection point between the mechanism and the back-support will be in its correspondence. Excluding the vertebra T1 (that is adjacent to the cervical region, and might cause interference between the device and the human's neck while bending), such vertebra is the one maximizing the support action of the device. The number of scissor units defining the mechanism and their size (*i.e.*, D parameter in Fig. 9), together with the L parameter (defining the length of the connection element between the scissor mechanism and the connection point in the correspondence of the reference vertebra T2) have been considered in the optimization problem. The following parameters ranges have been taken into account: scissor units $= [2, 5]$; $D = [37.5, 50]$ mm (step of 2.5 mm); $L = [350, 400]$ mm (step of 5 mm). The optimization problem has been implemented in Matlab, exploiting the scissor hinge kinematics formulation described in Section 3.3 and the *lsqnonlin* Matlab algorithm (Marquardt, 1963). Fig. 10 shows an iteration of the optimization procedure, highlighting the obtained mechanism path w.r.t. the approximated circular path of the reference vertebra T2. Once the optimization has been completed, the final configuration of the scissor hinge mechanism in Fig. 11 has been obtained. The optimized parameters for the specific user tracked in our experiment were: scissor units $=$ 3; $D = 45$ mm; $L = 380$ mm. The resulting mechanism is able to track the circular path related to the reference vertebra T2.

Remark 4. The design of the scissor hinge mechanism has to be performed for each specific user separately, computing the optimized mechanism elements sizes to be implemented on the tailored exoskeleton. The tailored user-based mechanism optimization exploits user-specific vertebrae motion data acquired as described in Section 2.2.2. Such user-specific data are used as reference, *i.e.*, the designed device must be able to follow the reference vertebrae motion of the specific user. Due to the simple and easily-implementable design of the mechanism, the scissor hinge elements can be designed (choosing the number of scissor units, and proper values of D and L) to track the reference

vertebra T2 motion for each specific user.

3.5. Static load analysis

In order to perform the static load analysis of the proposed mechanism, the actuation schema in Fig. 12 has been considered. The device has been considered actuated by a motor allowing for the positioning of the scissor hinge mechanism. The selected motor positioning allows minimizing the encumbrance of the parts and, therefore, the size of the device. Exploiting the *virtual work* principle (Antman and Osborn, 1979) it is possible to compute the static load acting on the mechanism:

$$\sum_i F_i \delta s_i + \sum_j C_j \delta \alpha_j + C_\alpha \delta \alpha = 0; \tag{4}$$

where F_i and δs_i represent the external i^{th} applied force and its virtual displacement respectively, C_j and $\delta \alpha_j$ represent the external i^{th} applied torque and its virtual rotation respectively, and C_α and $\delta \alpha$ represent the motor torque and its virtual rotation respectively. Substituting (3) into (4) (to obtain δs_i as a function of α):

$$\sum_i -F_i \delta(L\sin(\alpha + \vartheta') + D\sin(\alpha) + D\sin(\alpha)) - \sum_j C_j \delta \alpha_j + C_\alpha \delta \alpha = 0. \tag{5}$$

By deriving (5) w.r.t. $\delta \alpha$:

$$C_\alpha = \sum_i F_i(L\cos(\alpha + \vartheta') + 2D\cos(\alpha)) + \sum_j C_j. \tag{6}$$

The target scenario to perform the static load analysis was the same as described in the previous work (Mauri et al., 2019), in which a heavy part (*e.g.*, a car bumper) had to be manipulated. The maximum considered load was of 10 kg (considering both the human's arm weight and the part's weight). The considered reference human's arm configuration for the lifting and transportation of the part is shown in Fig. 13. The human was considered to transport the part in the reference (*i.e.*, nominal) configuration, in which the arm is vertical and the forearm is
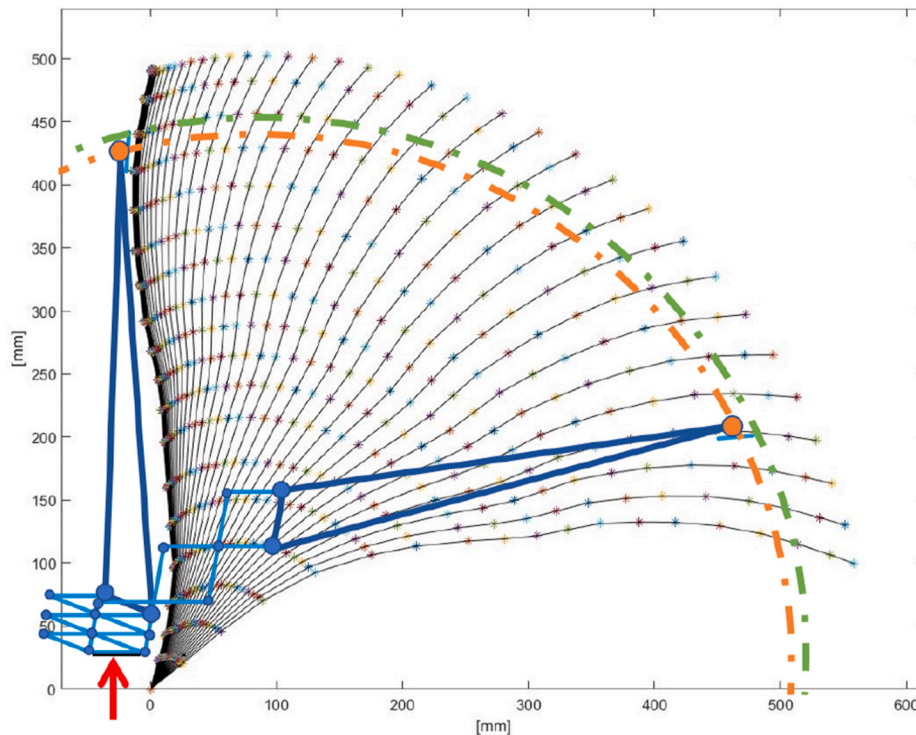
Fig. 10. Optimization iteration of the scissor hinge mechanism. The obtained mechanism motion path is compared with the one of the reference vertebra T2. The red arrow indicates the constraint between the designed mechanism and the lumbar fixing. (For interpretation of the references to colour in this figure legend, the reader is referred to the Web version of this article.)
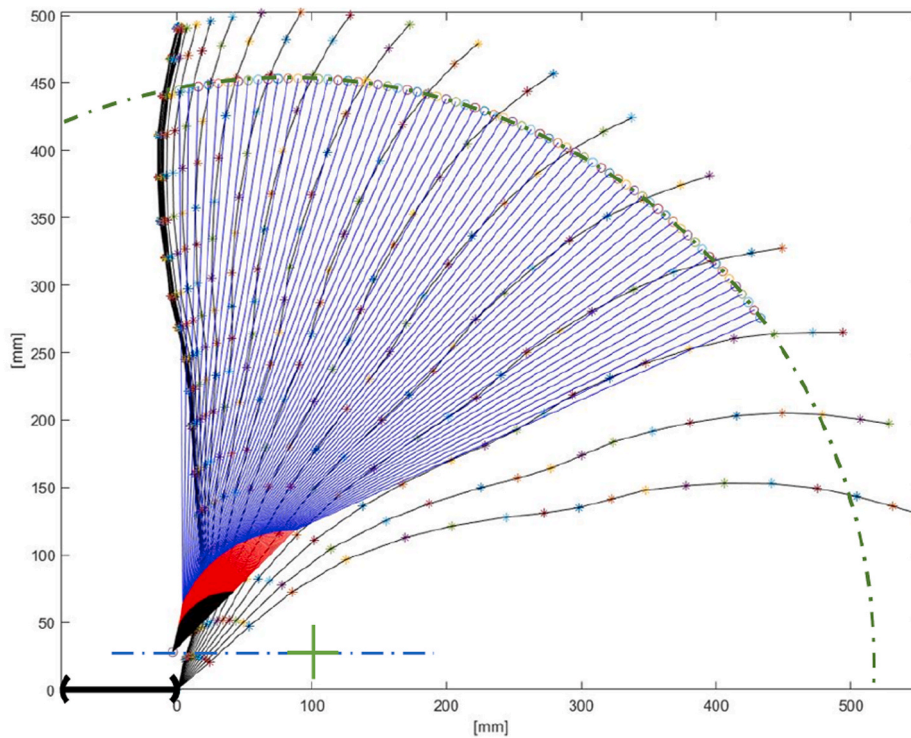
Fig. 11. Optimized scissor hinge mechanism. The final designed mechanism is able to track the approximated circular path of the reference vertebra T2.
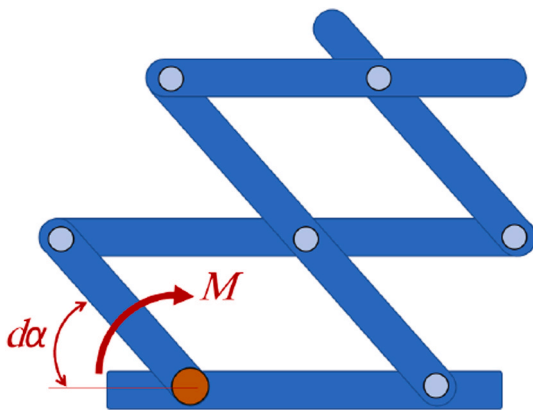
Fig. 12. Actuation schema.

perpendicular to the arm. The distance d_{load} in Fig. 13 is the one between the center of mass of the manipulated part and the reference vertebra connection point.

Considering the scenario proposed in Fig. 13, the resulting load schema is shown in Fig. 14 (left side), where the applied vertical force is
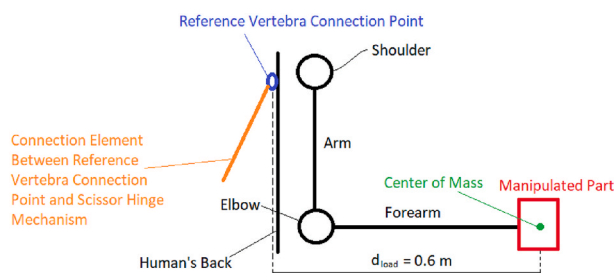
Fig. 13. Reference human's arm configuration for the considered lifting and transportation task.

equal to 100 N (*i.e.*, 10 kg multiplied by the gravity acceleration) and the resulting torque is 60 Nm (*i.e.*, 100 N multiplied by the distance d_{load}). The resulting required motor torque C_α is shown in Fig. 14 (right side) as a function of α.

3.6. Commercial parts for actuation implementation

In order to actuate the proposed device, the following commercial gear-motors have been considered as possible solutions (exploiting the static load analysis performed in Section 3.5): option #1 EC60 Maxon motor equipped by the planetary gear GP81; option #2 gear-motor Harmonic Drive SHA-SG 20A. Both the selected gear-motors are DC motors, thus it is possible to power them using a battery installed directly on the exoskeleton. The size and weight of the battery can be selected on the basis of the foreseen target operative time and on the basis of the maximum desired weight/size for the designed device.

3.7. Prototype

On the basis of the described design, the final CAD model of the proposed back-support exoskeleton is shown in Fig. 15. The scissor hinge mechanism (blue) adopted to track the motion of the reference vertebra T2 is mounted on a lumbar support (gray). The motor (red) to actuate the mechanism is highlighted. The terminal part of the scissor hinge mechanism is connected to the back-support (green).

The proposed designed device has been 3D-printed. The printed prototype did not include the actuation system. The printed device has been realized in order to show its simple implementation and manufacturing. In addition, exploiting the realized prototype, it was possible to briefly evaluate its achieved functionalities. Fig. 16 shows the adaptability of the device to the user posture. Fig. 17 shows the simulation of a lifting task adopting the proposed device.

Preliminary evaluation of the proposed design on the basis of the approach proposed in (Van der Grinten and Smitt, 1992) has been performed. The main aim of the evaluation was to analyze the perceived discomfort while wearing the device and executing a lifting task (as in
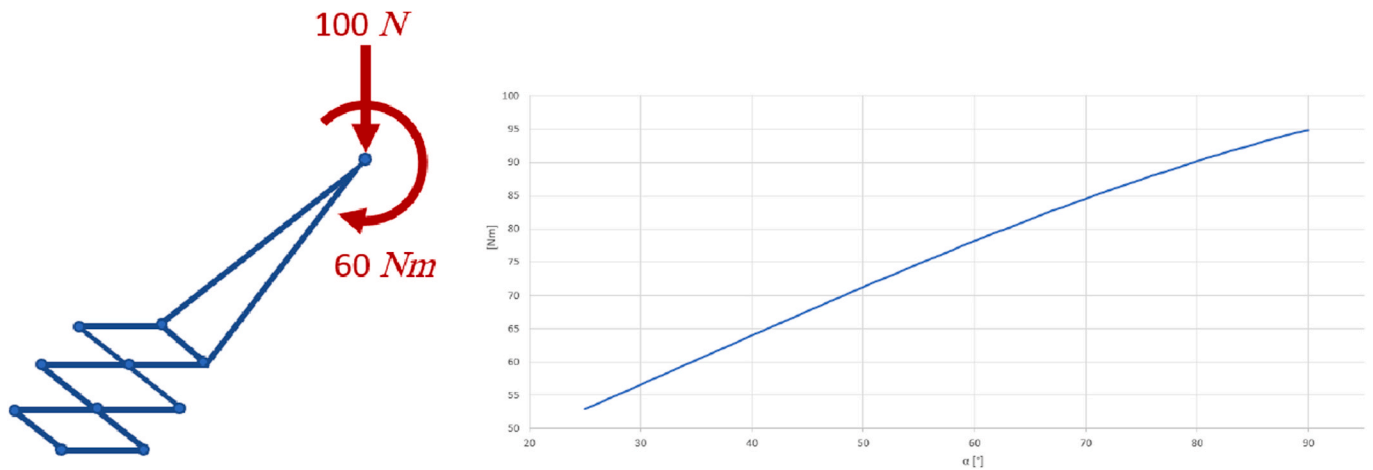
Fig. 14. Load scenario (left side). Required motor torque C_α (right side).
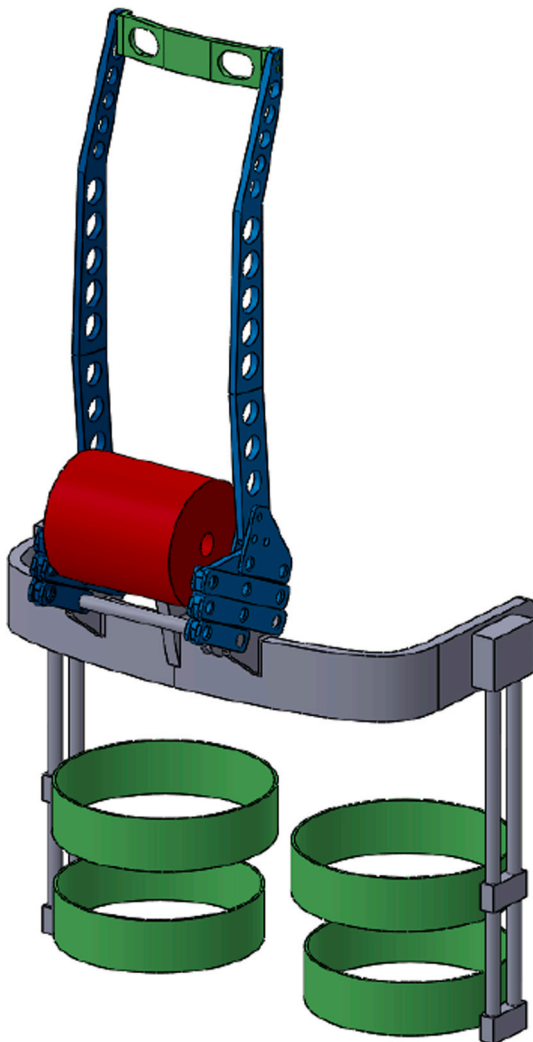
Fig. 15. Final CAD of the designed prototype of the back-support exoskeleton with backbone-based kinematics enhanced by the scissor hinge mechanism.

Fig. 17), to verify the validity of the proposed design methodology. The goal was, therefore, to verify that no limitations to the human motion were caused by the device, *i.e.*, not requiring the implementation of the actuation system. The evaluation protocol consisted in 10 lifting tasks,

executed three times. After each execution, the questionnaire in (Van der Grinten and Smitt, 1992) has been filled, judging the discomfort in the following body areas: neck, upper back (left side), upper back (right side), lower back (left side), lower back (right side), buttock (left side), buttock (right side). A scale between 0 (no discomfort at all) and 10 (extreme discomfort) has been considered to judge the perceived discomfort. The obtained results are detailed in Table 1, highlighting that the proposed design is suitable. Future work will extensively investigate the full performance of the device considering a subjects-based optimization, realization and testing of the prototype.

Remark 5. The proposed device (based on the easily scissor hinge mechanism) allows being adapted to different users on the basis of the proposed tailored design (*i.e.*, changing the size of the mechanism's elements to track the reference motion of the specific user's backbone - Section 2.2). In addition, its simple mechanical design allows to reduce the costs, the size and the dimensions of the device, making its engineering process easy.

Remark 6. The here proposed evaluation of the device is described in order to validate the performance of the proposed design methodology in a preliminary way. In fact, in the case that the prototype would have resulted in an unsatisfactory design, all the design methodology should have been reviewed. The here described evaluation wants to lay the basis for the next validation phase, in which the device will be optimized, fully realized (*i.e.*, including all the components and actuation system), and tested for a larger number of users (at least 10 subjects with different age, sex and anthropometric characteristics).

4. Conclusions and current and future work

The proposed work described the design methodology for an active back-support exoskeleton with backbone-based kinematics. Exploiting a scissor hinge mechanism, the proposed device allows to track the motion of a reference vertebra, in order to adapt its configuration to the human posture while executing a task. Due to the simple implementation and to the tailored design, the proposed mechanism can be easily re-optimized to be adapted to the anthropometric measures of each specific human operator. A prototype has been 3D-printed. A preliminary analysis of the capabilities of the device has been performed, highlighting its suitable design.

The main limitation of the here presented work is related to the fact that only one subject has been considered for validating the modeling of the backbone kinematics. However, since the mechanism design is customized for the specific user, the study can be easily extended to more subjects.

Current and future works are devoted to implement the actuated
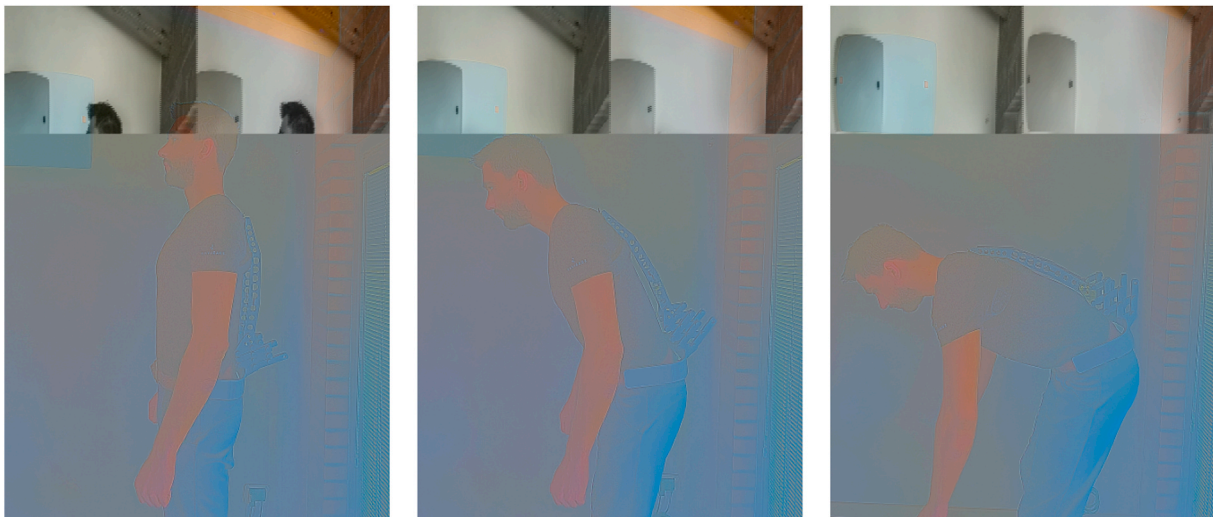
Fig. 16. Adaptability of the proposed device to the user posture.

Fig. 17. Simulated lifting task adopting the proposed device.

Table 1
Discomfort evaluation on the basis of (Van der Grinten and Smitt, 1992).

	task #1	task #2	task #3
Neck	0	0	0
upper back (left side)	2	2	2
upper back (right side)	2	2	2
lower back (left side)	0	0	0
lower back (right side)	0	0	0
buttock (left side)	2	2	2
buttock (right side)	2	2	2

version of the exoskeleton, and to study a possible extension of the available DoFs of the device (*e.g.*, implementing a three rotational DoFs device (Marras et al., 1992; Beil and Asfour, 2016)). In fact, while the current design already foresees the adoption of elastic elements enabling limited lateral flexion and axial rotation (as detailed in Section 2.2), the proposed device does not allow to sweep out the complete achievable motion of the backbone. To achieve this goal, the adopted model to describe the backbone kinematics will be updated including all the rotational DoFs, properly adjusting the device design. Control strategies are currently under investigation to provide assistance as it is required.

Moreover, extensive tests of the proposed device are foreseen as stated in Section 3.7. In addition to the protocol described in (Van der Grinten and Smitt, 1992), such tests can be based also on the protocols described in Godwin et al. (2009); Sylla et al. (2014); Whitfield et al. (2014); Toxiri et al. (2017b); Huysamen et al. (2018b) to have a wider analysis of the performance.

Declaration of competing interest

The authors declare that they have no known competing financial interests or personal relationships that could have appeared to influence the work reported in this paper.

Acknowledgment

Appendix A. Supplementary data

Supplementary data to this article can be found online at https://doi.org/10.1016/j.ergon.2020.102991.

References

Aldak, 2020. https://exoskeletonreport.com/product/aldak-passive/. (Accessed 1 March 2020).

Antman, S.S., Osborn, J.E., 1979. The principle of virtual work and integral laws of motion. Arch. Ration. Mech. Anal. 69 (3), 231–262.

Atlas, 2020. https://exoskeletonreport.com/product/atlas/. (Accessed 1 March 2020).

Awn, 2020. https://exoskeletonreport.com/product/awn-03/. (Accessed 1 March 2020).

Backx, 2020. https://exoskeletonreport.com/product/backx/. (Accessed 1 March 2020).

Baltrusch, S., Van Dieën, J., Van Bennekom, C., Houdijk, H., 2018. The effect of a passive trunk exoskeleton on functional performance in healthy individuals. Appl. Ergon. 72, 94–106.

Baltrusch, S., van Dieën, J., Koopman, A., Näf, M., Rodriguez-Guerrero, C., Babič, J., Houdijk, H., 2020. Spexor passive spinal exoskeleton decreases metabolic cost during symmetric repetitive lifting. Eur. J. Appl. Physiol. 120 (2), 401–412.

Bao, S., Howard, N., Lin, J.-H., 2020. Are work-related musculoskeletal disorders claims related to risk factors in workplaces of the manufacturing industry? Ann. Work Expo. Health 64 (2), 152–164.

Bazrgari, B., Shirazi-Adl, A., Arjmand, N., 2007. Analysis of squat and stoop dynamic liftings: muscle forces and internal spinal loads. Eur. Spine J. 16 (5), 687–699.

Beil, J., Asfour, S., 2016. New mechanism for a 3 dof exoskeleton hip joint with five revolute and two prismatic joints. In: 2016 6th IEEE International Conference on Biomedical Robotics and Biomechatronics (BioRob). IEEE, pp. 787–792.

Blanco, A., Catalán, J.M., Díez, J.A., García, J.V., Lledó, L.D., Lobato, E., García-Aracil, N.M., 2019. Advantages of the incorporation of an active upper-limb exoskeleton in industrial tasks. In: Iberian Robotics Conference. Springer, pp. 477–484.

Bogue, R., 2018. Exoskeletons – a review of industrial applications. Ind. Robot 45 (5), 585–590. https://doi.org/10.1108/IR-05-2018-0109.

Boocock, M., Naudé, Y., Taylor, S., Kilby, J., Mawston, G., 2019. Influencing lumbar posture through real-time biofeedback and its effects on the kinematics and kinetics of a repetitive lifting task. Gait Posture 73, 93–100.

Bosch, T., van Eck, J., Knitel, K., de Looze, M., 2016. The effects of a passive exoskeleton on muscle activity, discomfort and endurance time in forward bending work. Appl. Ergon. 54, 212–217.

Bragança, S., Costa, E., Castellucci, I., Arezes, P.M., 2019. A brief overview of the use of collaborative robots in industry 4.0: human role and safety. In: Occupational and Environmental Safety and Health. Springer, pp. 641–650.

Chen, Y., Fan, L., Feng, J., 2017. Kinematic of symmetric deployable scissor-hinge structures with integral mechanism mode. Comput. Struct. 191, 140–152.

Comau mate, 2020. https://www.comau.com/EN/our-competences/robotics/Exoskeleton. (Accessed 1 March 2020).

De Looze, M.P., Bosch, T., Krause, F., Stadler, K.S., O'Sullivan, L.W., 2016. Exoskeletons for industrial application and their potential effects on physical work load. Ergonomics 59 (5), 671–681.

Exobionics, 2020. https://eksobionics.com/eksoworks/. (Accessed 1 March 2020).

Flx-ergoskeleton, 2020. https://exoskeletonreport.com/product/flx-ergoskeleton/. (Accessed 1 March 2020).

Godwin, A.A., Stevenson, J.M., Agnew, M.J., Twiddy, A.L., Abdoli-Eramaki, M., Lotz, C. A., 2009. Testing the efficacy of an ergonomic lifting aid at diminishing muscular fatigue in women over a prolonged period of lifting. Int. J. Ind. Ergon. 39 (1), 121–126.

Guncan, B., Unal, R., 2018. Ant-m: design of passive lower-limb exoskeleton for weight-bearing assistance in industry. In: International Symposium on Wearable Robotics. Springer, pp. 500–504.

h-wex, 2020. https://exoskeletonreport.com/product/h-wex/. (Accessed 1 March 2020).

Hal lumbar support. https://exoskeletonreport.com/product/hal-for-lumbar-support/. (Accessed 1 March 2020).

Hensel, R., Keil, M., 2019. Subjective evaluation of a passive industrial exoskeleton for lower-back support: a field study in the automotive sector. IISE Trans. Occup. Ergon. Hum. Factors 1–9.

Hentout, A., Aouache, M., Maoudj, A., Akli, I., 2019. Human–robot interaction in industrial collaborative robotics: a literature review of the decade 2008–2017. Adv. Robot. 33 (15–16), 764–799.

Huysamen, K., Power, V., O'Sullivan, L., 2018a. Elongation of the surface of the spine during lifting and lowering, and implications for design of an upper body industrial exoskeleton. Appl. Ergon. 72, 10–16.

Huysamen, K., de Looze, M., Bosch, T., Ortiz, J., Toxiri, S., O'Sullivan, L.W., 2018b. Assessment of an active industrial exoskeleton to aid dynamic lifting and lowering manual handling tasks. Appl. Ergon. 68, 125–131.

Hyundai vex, 2020. https://www.hyundai.news/eu/brand/hyundai-develops-wearable-vest-exoskeleton-for-overhead-work/. (Accessed 1 March 2020).

Ibrahim, M.E., Weber, K., Courvoisier, D.S., Genevay, S., 2019. Recovering the capability to work among patients with chronic low back pain after a four-week, multidisciplinary biopsychosocial rehabilitation program: 18-month follow-up study. BMC Muscoskel. Disord. 20 (1), 439.

Katz, J.N., 2006. Lumbar disc disorders and low-back pain: socioeconomic factors and consequences. JBJS 88 (Suppl. l_2), 21–24.

Ko, H.K., Lee, S.W., Koo, D.H., Lee, I., Hyun, D.J., 2018. Waist-assistive exoskeleton powered by a singular actuation mechanism for prevention of back-injury. Robot. Autonom. Syst. 107, 1–9.

Koopman, A.S., Kingma, I., Faber, G.S., de Looze, M.P., van Dieën, J.H., 2019. Effects of a passive exoskeleton on the mechanical loading of the low back in static holding tasks. J. Biomech. 83, 97–103.

Laevo v2, 2020. https://exoskeletonreport.com/product/laevo/. (Accessed 1 March 2020).

Lanotte, F., Grazi, L., Chen, B., Vitiello, N., Crea, S., 2018. A low-back exoskeleton can reduce the erector spinae muscles activity during freestyle symmetrical load lifting tasks. In: 7th IEEE International Conference on Biomedical Robotics and Biomechatronics (Biorob), IEEE, 2018, pp. 701–706.

Li, P.L., Achiche, S., Blanchet, L., Lecours, S., Raison, M., 2019. Design of an Assistive Trunk Exoskeleton Based on Multibody Dynamic Modelling. arXiv preprint arXiv: 1910.01184.

Liu, Y., Xiao, L., Zhou, H., Xie, C., Huang, L., 2019a. An analysis of work-related musculoskeletal disorders and ergonomic loads in male welders in shipbuilding industry. Chin. J. Ind. Hyg. Occup. Dis. (Zhonghua lao dong wei sheng zhi ye bing za zhi) 37 (3), 201–206.

Liu, Q., Liu, Z., Xu, W., Tang, Q., Zhou, Z., Pham, D.T., 2019b. Human-robot collaboration in disassembly for sustainable manufacturing. Int. J. Prod. Res. 57 (12), 4027–4044.

Lockheed martin, 2020. https://www.lockheedmartin.com/. (Accessed 1 March 2020).

Lu, Y., 2017. Industry 4.0: a survey on technologies, applications and open research issues. J. Ind. Inf. Integrat. 6, 1–10.

Luger, T., Cobb, T.J., Seibt, R., Rieger, M.A., Steinhilber, B., 2019. Subjective evaluation of a passive lower-limb exoskeleton used during simulated assembly. IISE Trans. Occup. Ergon. Hum. Factors 1–10.

Maden, F., Korkmaz, K., Akgün, Y., 2011. A review of planar scissor structural mechanisms: geometric principles and design methods. Architect. Sci. Rev. 54 (3), 246–257.

Madinei, S., Alemi, M.M., Kim, S., Srinivasan, D., Nussbaum, M.A., 2020. Biomechanical Evaluation of Passive Back-Support Exoskeletons in a Precision Manual Assembly Task:"expected" Effects on Trunk Muscle Activity, Perceived Exertion, and Task Performance, Human Factors, 0018720819890966.

Manns, P., Sreenivasa, M., Millard, M., Mombaur, K., 2017. Motion optimization and parameter identification for a human and lower back exoskeleton model. IEEE Robot. Autom. Lett. 2 (3), 1564–1570.

Marquardt, D.W., 1963. An algorithm for least-squares estimation of nonlinear parameters. J. Soc. Ind. Appl. Math. 11 (2), 431–441.

Marras, W., Fathallah, F., Miller, R., Davis, S., Mirka, G., 1992. Accuracy of a three-dimensional lumbar motion monitor for recording dynamic trunk motion characteristics. Int. J. Ind. Ergon. 9 (1), 75–87.

Mauri, A., Lettori, J., Fusi, G., Fausti, D., Mor, M., Braghin, F., Legnani, G., Roveda, L., 2019. Mechanical and control design of an industrial exoskeleton for advanced human empowering in heavy parts manipulation tasks. Robotics 8 (3), 65.

Muscle suit, 2020. https://exoskeletonreport.com/product/muscle-suit/. (Accessed 1 March 2020).

Näf, M.B., Koopman, A.S., Baltrusch, S., Rodriguez-Guerrero, C., Vanderborght, B., Lefeber, D., 2018. Passive back support exoskeleton improves range of motion using flexible beams. Front. Robot. AI 5, 72.

Naruse, K., Kawai, S., Yokoi, H., Kakazu, Y., 2003. Development of wearable exoskeleton power assist system for lower back support. In: Proceedings 2003 IEEE/RSJ International Conference on Intelligent Robots and Systems (IROS 2003)(Cat. No. 03CH37453), vol. 4. IEEE, pp. 3630–3635.

Pacifico, I., Scano, A., Guanziroli, E., Moise, M., Morelli, L., Chiavenna, A., Romo, D., Spada, S., Colombina, G., Molteni, F., Giovacchini, F., Vitiello, N., Crea, S., 2020. Experimental evaluation of the proto-mate: a novel ergonomic upper-limb exoskeleton for reducing the worker's physical strain. IEEE Robot. Autom. Mag. https://doi.org/10.1109/MRA.2019.2954105, 0–0.

Roveda, L., Ghidoni, S., Cotecchia, S., Pagello, E., Pedrocchi, N., 2017. Eureca h2020 cleansky 2: a multi-robot framework to enhance the fourth industrial revolution in the aerospace industry. In: Robotics and Automation (ICRA), 2017 IEEE Int Conf on, Workshop on Industry of the Future: Collaborative, Connected, Cognitive. Novel Approaches Stemming from Factory of the Future and Industry, vol. 4, 0 initiatives.

Shin, H.-J., Kim, J.-Y., 2007. Measurement of trunk muscle fatigue during dynamic lifting and lowering as recovery time changes. Int. J. Ind. Ergon. 37 (6), 545–551.

Spada, S., Ghibaudo, L., Gilotta, S., Gastaldi, L., Cavatorta, M.P., 2017. Investigation into the applicability of a passive upper-limb exoskeleton in automotive industry. Procedia Manuf. 11, 1255–1262.

Suitx, 2020. https://www.suitx.com/. (Accessed 1 March 2020).

Sylla, N., Bonnet, V., Colledani, F., Fraisse, P., 2014. Ergonomic contribution of able exoskeleton in automotive industry. Int. J. Ind. Ergon. 44 (4), 475–481.

Toxiri, S., Ortiz, J., Masood, J., Fernández, J., Mateos, L.A., Caldwell, D.G., 2017a. A powered low-back exoskeleton for industrial handling: considerations on controls. In: Wearable Robotics: Challenges and Trends. Springer, pp. 287–291.

Toxiri, S., Ortiz, J., Caldwell, D.G., 2017b. Assistive strategies for a back support exoskeleton: experimental evaluation. In: International Conference on Robotics in Alpe-Adria Danube Region. Springer, pp. 805–812.

V22 ergoskeleton, 2020. https://exoskeletonreport.com/product/v22-ergoskeleton/. (Accessed 1 March 2020).

Van der Grinten, M.P., Smitt, P., 1992. Development of a practical method for measuring body part discomfort. Adv. Ind. Ergon. Saf. 4, 311–318.

Vicentini, F., Pedrocchi, N., Beschi, M., Giussani, M., Iannacci, N., Magnoni, P., Pellegrinelli, S., Roveda, L., Villagrossi, E., Askarpour, M., et al., 2020. Piros: cooperative, safe and reconfigurable robotic companion for cnc pallets load/unload

stations. In: Bringing Innovative Robotic Technologies from Research Labs to Industrial End-Users. Springer, pp. 57–96.

Vicon camera system. https://www.vicon.com/hardware/cameras/. (Accessed 1 March 2020).

Wang, X., Dong, X.S., Choi, S.D., Dement, J., 2017. Work-related musculoskeletal disorders among construction workers in the United States from 1992 to 2014. Occup. Environ. Med. 74 (5), 374–380.

Wehner, M., Rempel, D., Kazerooni, H., 2009. Lower extremity exoskeleton reduces back forces in lifting. In: ASME 2009 Dynamic Systems and Control Conference. American Society of Mechanical Engineers Digital Collection, pp. 49–56.

Whitfield, B.H., Costigan, P.A., Stevenson, J.M., Smallman, C.L., 2014. Effect of an on-body ergonomic aid on oxygen consumption during a repetitive lifting task. Int. J. Ind. Ergon. 44 (1), 39–44.

Wijegunawardana, I., Kumara, M., De Silva, H., Viduranga, P., Ranaweera, R., Gopura, R., Madusanka, D., 2019. Chairx: a robotic exoskeleton chair for industrial workers. In: IEEE 16th International Conference on Rehabilitation Robotics (ICORR), IEEE, 2019, pp. 587–592.

Yang, C., Virk, G., Yang, H., 2017. Wearable Sensors and Robots.

Yang, X., Huang, T., Hu, H., Yu, S., Zhang, S., Zhou, X., Carriero, A., Yue, G., Su, H., 2019. Spine-inspired continuum soft exoskeleton for stoop lifting assistance. IEEE Robot. Autom. Lett. 4 (4), 4547–4554. https://doi.org/10.1109/LRA.2019.2935351.

Zhang, T., Huang, H., 2018. A lower-back robotic exoskeleton: industrial handling augmentation used to provide spinal support. IEEE Robot. Autom. Mag. 25 (2), 95–106. https://doi.org/10.1109/MRA.2018.2815083.